Sensing external spins with nitrogen-vacancy diamond

2011 New J. Phys. 13 055004

(http://iopscience.iop.org/1367-2630/13/5/055004)

New Journal of Physics
The open-access journal for physics

Sensing external spins with nitrogen-vacancy diamond

Bernhard Grotz[1], Johannes Beck[1], Philipp Neumann[1], Boris Naydenov[1], Rolf Reuter[1], Friedemann Reinhard[1], Fedor Jelezko[1], Jörg Wrachtrup[1], David Schweinfurth[2], Biprajit Sarkar[2] and Philip Hemmer[3,4]

[1] Physikalisches Institut and Research Center SCoPE, Universität Stuttgart, Stuttgart 70550, Germany
[2] Institut für Anorganische Chemie, Universität Stuttgart, Stuttgart 70550, Germany
[3] Electrical and Computer Engineering, Texas A&M University, College Station, TX 77843, USA
E-mail: prhemmer@ece.tamu.edu

New Journal of Physics **13** (2011) 055004 (7pp)
Received 16 January 2011
Published 19 May 2011
Online at http://www.njp.org/
doi:10.1088/1367-2630/13/5/055004

Abstract. A single nitrogen-vacancy (NV) center is used to sense individual, as well as small ensembles of, electron spins placed outside the diamond lattice. Applying double electron–electron resonance techniques, we were able to observe Rabi nutations of these external spins as well as the coupling strength between the external spins and the NV sensor, via modulations and accelerated decay of the NV spin echo. Echo modulation frequencies as large as 600 kHz have been observed, being equivalent to a few nanometers distance between the NV and an unpaired electron spin. Upon surface modification, the coupling disappears, suggesting the spins to be localized at surface defects. The present study is important for understanding the properties of diamond surface spins so that their effects on NV sensors can eventually be mitigated. This would enable potential applications such as the imaging and tracking of single atoms and molecules in living cells or the use of NVs on scanning probe tips to entangle remote spins for scalable room temperature quantum computers.

[4] Author to whom any correspondence should be addressed.

For many applications, the ability to sense and image single electron and nuclear spins in real time under ambient conditions would have unprecedented implications. For example, detailed changes in the structure and electron configuration of individual biomolecules such as proteins or DNA could be tracked in real time in living cells. For this reason, much excitement was generated when it was shown that the electron spin of a single nitrogen-vacancy (NV) color center is a highly sensitive probe able to detect the magnetic fields generated by single electron and nuclear spins [1, 2]. The NV spin can be mapped onto different fluorescence levels and therefore enables optically detected magnetic resonance (ODMR) experiments on a single NV defect [3]. As a result, a number of proposals have addressed methods to increase the sensitivity of diamond spin-based magnetometry [4–6]. In addition, the conditions for optimum imaging and sensitivity under realistic environmental conditions have been explored [7]. All experimental demonstrations so far have involved using the NV center's spin ($S = 1$) to sense electron and nuclear spins inside the same diamond crystal [8–10]. However, to be useful for most applications, the NV must detect spins that are external to the diamond lattice. Attempts to do this have so far been disappointing owing to the mostly short spin coherence lifetimes of the NVs near the surface either in nanocrystals [11] or in shallow implanted bulk diamond [12]. Here we show that under certain conditions it is possible to prepare the surface to be able to detect an individual electron spin or a spin bath on or near the surface, but outside the diamond lattice. Apart from being the first demonstration of external spin detection by NV diamond, these measurements also provide key information about the nature of diamond surface spins that can be used to mitigate their decoherence effects and thereby eventually enable the most exciting potential applications of single NV diamond magnetic sensors.

To detect external diamond spins, shallow NVs, estimated within a few nanometers of the surface, are created by using low-energy (2–5 keV per $^{15}N_2$) [13] nitrogen implantation in a (100)-diamond sample with low natural nitrogen concentration followed by annealing at 800 °C for 2 h in vacuum (figure 1(a)). The nearby spins are detected using double electron–electron resonance (DEER) [14] as illustrated in figures 1(b) and (c). Basically, this sequence consists of an NV spin echo (figures 1(b) and (c), top) that is sensitive to magnetic field changes during one of the free precession times τ. The magnetic field change is induced by rotating the nearby dark spin (figures 1(b) and (c), bottom) using a second microwave field tuned to its resonance frequency. Within such a setup, two types of experiments are possible. Rabi oscillations of the external spin can be driven by changing the length of the pulse on the coupled dark spin, as in figure 1(b). In this way, the strength of the magnetic field change is altered (maximum for a π pulse). Alternatively, sequences that flip the external spin by pulses of constant lengths are possible, as illustrated by the π pulse on the dark electron spin in figure 1(c). In this case, the timing of the dark spin π pulse relative to the final $\pi/2$ pulse is varied, and the echo reveals the total magnetic field generated by the dark spins. The key property of the DEER sequence is that it does not matter which state the dark spin is in initially since the NV echo amplitude will decrease in either case when the dark spin is flipped. It is, however, important that the spin lattice relaxation time (T_1) of the dark spin is comparable to or longer than the measurement time of the NV spin.

To provide proof that the detected spins are indeed surface spins and not inside the diamond crystal, the same NVs are probed after different surface preparations. A convenient way to functionalize the diamond surface is provided by silane chemistry as was already successfully demonstrated on bulk diamonds [15], ultrananocrystalline diamond surfaces [16] and nanodiamonds [17]. The eventual goal of such functionalization is to produce bio-specific

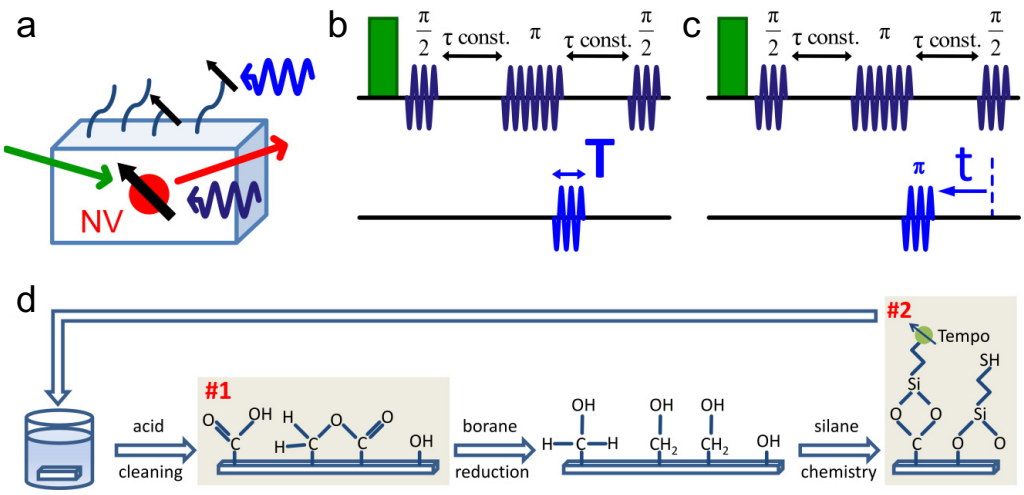

Figure 1. (a) NV spins (black arrow in red circle) in diamond are used to sense external spins (black arrows) on functionalized surfaces. Laser light (532 nm, green arrow) induces spin-dependent fluorescence (red arrow). Microwave radiation (wavy arrows) manipulates spins. (b) Pulse sequence for Rabi on an external electron spin. The green pulse denotes the optical pumping laser at 532 nm. The upper blue microwave pulses are resonant with the NV center spin (∼1.02 GHz in an axial ∼650 Gauss magnetic field) and perform a Hahn echo. The lower blue pulse, of varying length, is applied at the resonance frequency expected for an unpaired electron spin (1.85 GHz) in the present external magnetic field. (c) The DEER sequence on external spin. Here the dark spin pump pulse has a fixed area of π, but the time delay between it and the final NV $\pi/2$ pulse is varied. The NV echo pulse delays are kept constant. (d) Surface functionalization procedure.

fluorescent and magnetic probes. The most common surface preparations for the presented experiments were (1) acid cleaning by boiling the diamond in a 1 : 1 : 1 mixture of sulfuric, nitric and perchloric acids under reflux for at least 2 h and (2) a more complex surface functionalization starting with the acid-cleaned surface, followed by reducing the surface with borane, covalent binding of (3-Mercaptopropyl)methyldimethoxysilane (Aldrich) in THF and the spin-label 4-Maleimido-TEMPO (Aldrich) in turn, as illustrated in figure 1(d). In some cases, acid treatment was also performed to remove the functionalization on surface type 2, restoring it back to surface type 1.

When NVs are within a few nanometers of the diamond surface, short-spin coherence times are generally observed. Significantly, this coherence time is often sensitive to details of the surface preparation. In some cases returning the surface to its original state does reproduce the coherence time, which suggests that the NV is sensing local variations in spin density on the surface, for example as proposed for single NV scanning probe magnetometers [18]. However, for most of the NVs in this study the coherence time was too short to allow the application of a DEER pulse sequence, and therefore details of these interactions could not be determined. Of the NVs with long enough coherence time, some did not show sensitivity to the surface and this suggests that they were farther below the surface than the others. Although we could not directly measure implant depth, a certain fraction of the implanted NVs are expected to be farther from the surface due to the significant straggle of depths for low-energy implantation,

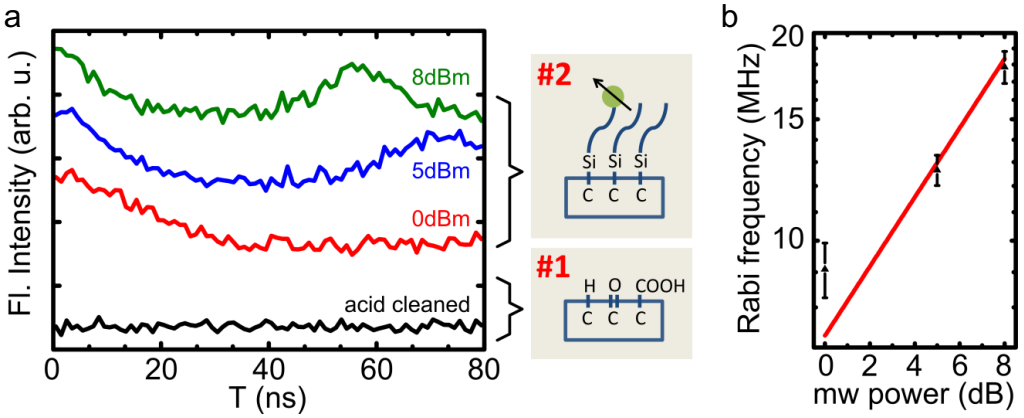

Figure 2. (a) Rabi oscillations on an unpaired electron spin next to a single NV center for a functionalized surface 2. The bottom trace shows no oscillations when the surface functionalization is removed (surface 1). This verifies that the oscillations are due to spins outside the diamond lattice. (b) Rabi oscillation frequencies depending on microwave power. The solid line is a fit showing square root dependence.

as predicted with SRIM simulations [19]. This assertion is also supported by the fact that NVs implanted with higher energies show no clear correlation between implant energy and coherence time. Remarkably, some shallow NV spins showed long enough coherence time for a DEER experiment, and the results are summarized below.

Figure 2 provides convincing proof that the dark spins we observe to interact with one of the NVs are in fact surface spins. Here the dark spins were driven by microwave pulses at frequencies where surface $S = 1/2$ spins are expected to respond ($g = 2$). Significantly, these oscillations are observed only on the functionalized surface 2 and are absent after the surface is acid cleaned to remove the functional groups. Evidence that these are Rabi oscillations is shown by the dependence of oscillation frequency on the microwave power. The distorted sinusoidal shape of the oscillations (similar to revivals) suggests that there is more than one external spin being driven in this case. Also owing to the limited T_2 time of the NV, only a fraction or a single Rabi cycle could be observed.

For several individual NVs that had a long enough echo T_2 decay time, the DEER delay sequences of figure 1(c) were applied as shown in figure 3(c). When the resonance frequency of the observer spin (NV) and the pumped spin (surface spin) are well separated such that the surface spins can be driven separately, the application of a π pulse at the frequency of the surface spin transition leads to a phase accumulation of the NV spin signal of $\Delta\phi_{ee} = \omega_{ee}t$, where ω_{ee} is the interaction of the NV and surface spin. When the dark spin pump pulse is very near the final $\pi/2$ pulse in the NV echo sequence (i.e. small t, see figure 1(c)), the signal is at a maximum since the static magnetic field shift caused by all the dark spins is canceled. As t increases, the DEER signal gives specific information about the coupling between the NV spin and those spins in the environment that are resonant with the dark spin π pulse. In the absence of exchange interaction [14], the spin-echo signal for pairs of spins (observer $= i$, pump $= k$) is governed by the dipolar interaction,

$$V(t) = V_0 \prod_{k \neq i} [1 - \lambda_k (1 - \cos(\omega_{ik} t))], \tag{1}$$

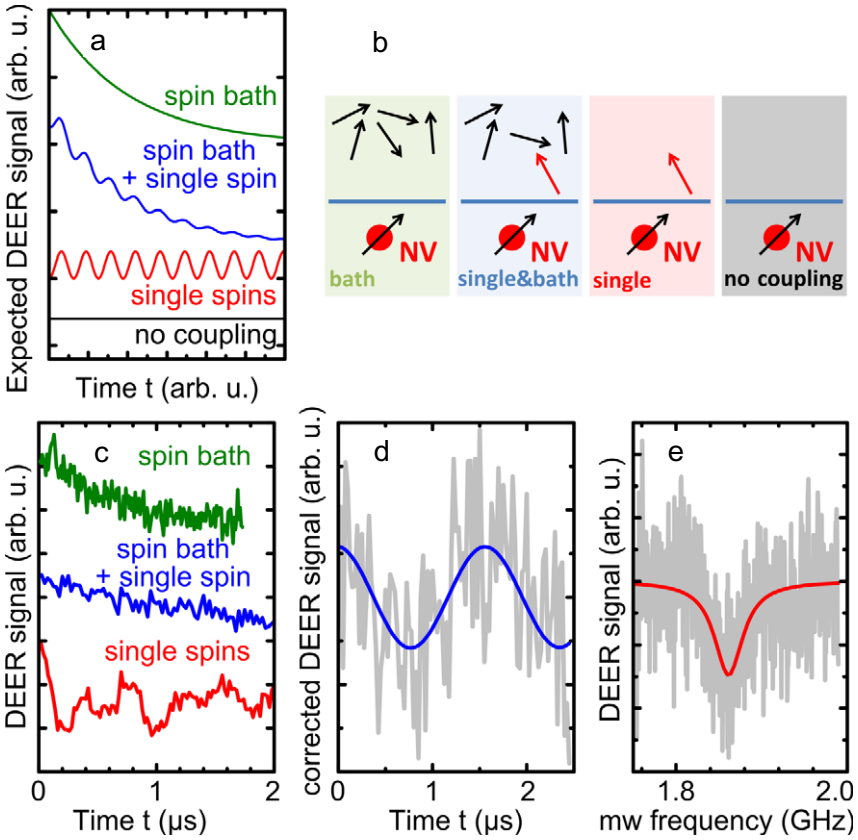

Figure 3. (a) Theoretical expected DEER curves for coupling to a spin bath (green), a spin bath with a dominant single spin (blue), a single spin without a spin bath (red) and no coupling to any spin (black). (b) Sketches of the aforementioned cases. (c) Experimental measurements of the cases of coupling to one or many external spins. (d) Decay corrected (exponential background subtracted) DEER signal of coupling to a spin bath with one pronounced spin (blue curve in figure 3(c)). The coupling frequency is 630 kHz, which corresponds to a distance of ∼3.5 nm. (e) ODMR spectra of the dark spins. The lack of a hyperfine structure suggests free or loosely bound electron spins.

with λ_k as the probability of flipping the dark spin with the π pulse and the dipolar interaction frequency

$$\omega_{ik} = \frac{\mu_0}{4\pi\hbar}\frac{g_i g_k \mu_B^2}{r_{ik}^3}(3\cos^2\theta_{ik} - 1). \tag{2}$$

Here the observer spin i is an NV ($g_i = 2$) and the pumped spin k is a dark electron spin ($g_k = 2$), while θ_{ik} is the angle between the magnetic field and the vector between the spins. Although this equation is strictly valid only for spin-1/2 it is also valid in the present case where the external magnetic field is applied along the NV quantization axis and is stronger than the effective field at the NV due to the dark spins. If the full spin triplet character of the NV is exploited, ω_{ik} will be twice as large [8]. The situation changes for a multi-spin system as there are contributions from many spins. For example, the signal changes to an exponential decay for an isotropic disordered

system, where the decay time T_{hom} is dependent on the local dark spin concentration [14],

$$V(t) = V_0 \exp(-t/T_{\mathrm{hom}}), \tag{3}$$

with the time constant

$$T_{\mathrm{hom}} = \frac{9\sqrt{3\hbar}}{2\pi g^2 \mu_{\mathrm{B}}^2 \mu_0 \lambda C}. \tag{4}$$

In the general case where there is both an isotropic spin bath plus individual (or localized clusters) of spins, the signal becomes a product of these two curves. Theoretically expected and experimental results for the cases of coupling to single spins and to spin baths are given in figures 3(a)–(c). In most cases the DEER sequences show just decay in the recorded signals (green curves). This is expected if the DEER pump pulse drives either a large ensemble of dark spins or a few diffusing spins. The decay time allows estimation of the concentration of the dark spins, which in the case of figure 3(c) is around 10^{14}–$10^{15}\,\mathrm{cm}^{-3}$ when we assume that T_1 of the surface spins are longer than the μs time window used here. Additionally, we would like to note that the decay characteristics of $V(t)$ depend on the dimensionality of the spin bath as $V(t) = V_0 \exp(-t/T_{\mathrm{hom}})^{d/3}$ with $d = 1, 2, 3$ depending on the dark spin distribution [20]. More importantly however, the DEER-induced decay sometimes shows a modulation that is caused by one or two non-diffusing spins with outstanding couplings ω_{ik}. While these oscillations can be pronounced for some centers (red curves), it is often necessary to subtract the exponential contribution of the spin bath to clearly see them (as for the blue curve in figure 3(c) that yields figure 3(d)). The oscillation frequency is a function of the dark spin distance γ_{ik} from the NV and its relative orientation θ_{ik}.

To determine the nature of the driven spin, ODMR spectra of the dark spins were taken as shown in figure 3(e). Here, the DEER signal was monitored while the pump pulse frequency was scanned. In this way, the resonance frequency of the dark spin can be determined. Since the applied magnetic field is known, this can be used to determine the spin g-factor. The measurement reveals an unpaired electron with $S = 1/2$ and $g = 2.015 \pm 0.005$ as the dark spin. It is worth mentioning that radicals on the diamond crystal surface have been found to show g values of $g = 2.0025$–2.0027 [21, 22]. Recently, a number of experiments on the unpaired electron spin in diamond nanocrystals have been published [23, 24]. Here similar values of the g-factor are found. Further identification of the coupled dark spin would require the observation of the hyperfine structure. Hyperfine coupling reveals the electron spin density distribution and the nature of the surrounding nuclei. A good example would be the hyperfine triplet seen for ^{14}N nuclei. In the case of paramagnetic nitrogen in the diamond lattice, the characteristic splitting would be $\approx$114 MHz [25]. As seen in figure 3(e), the observed spin does not show any hyperfine structure, which is typical for surface radicals from e.g. broken carbon σ-bonds, which are one of the most abundant diamond surface dangling bonds. This is also consistent with the notion that electron diffusion on the surface might be responsible for most of the observed decoherence.

In summary, we have observed single as well as ensembles of dark spins outside a diamond crystal using an NV magnetic sensor. We also identified the source of decoherence of NVs close to the diamond surface as unpaired electrons that may be ensembles or diffusing individuals. The fact that it was possible to immobilize some of these dark spins suggests that proper diamond surface functionalization will eventually enable the NV sensor to find successful application as a probe of electron and nuclear spins in molecules that are near the diamond surface, for example in living cells. Furthermore, when combined with scanning probe techniques, a diamond-based

spin sensor can be applied for imaging applications enabling the reconstruction of the three-dimensional structure of single biomolecules. The sensitivity of these devices can be further improved using dynamical decoupling pulse sequences as recently demonstrated for echo-based ac magnetic field sensing [26, 27].

Acknowledgment

This work was sponsored by DARPA QuEST, NIH, Internationale Spitzenforschung of the Baden-Württemberg Stiftung and the EU project Dinamo.

References

[1] Maze J R *et al* 2008 *Nature* **455** 644–7
[2] Balasubramanian G *et al* 2008 *Nature* **455** 648–51
[3] Gruber A, Drabenstedt A, Tietz C, Fleury L, Wrachtrup J and von Borczyskowski C 1997 *Science* **276** 2012–14
[4] Meriles C A, Jiang L, Goldstein G, Hodges J S, Maze J, Lukin M D and Cappellaro P 2010 *J. Chem. Phys.* **133** 124105
[5] Hall L T, Cole J H, Hill C D and Hollenberg L C L 2009 *Phys. Rev. Lett.* **103** 220802
[6] Cappellaro P and Lukin M D 2009 *Phys. Rev.* A **80** 032311
[7] Hall L T, Hill C D, Cole J H, Stadler B, Caruso F, Mulvaney P, Wrachtrup J and Hollenberg L C L 2010 *Proc. Natl Acad. Sci. USA* **107** 18777–82
[8] Neumann P *et al* 2010 *Nat. Phys.* **6** 249–53
[9] Jelezko F, Gaebel T, Popa I, Domhan M, Gruber A and Wrachtrup J 2004 *Phys. Rev. Lett.* **93** 130501
[10] Gaebel T *et al* 2006 *Nat. Phys.* **2** 408–13
[11] Tisler J *et al* 2009 *ACS Nano* **3** 1959–65
[12] Naydenov B, Reinhard F, Lämmle A, Richter V, Kalish R, D'Haenens-Johansson U F S, Newton M, Jelezko F and Wrachtrup J 2010 *Appl. Phys. Lett.* **97** 242511
[13] Pezzagna S, Wildanger D, Mazarov P, Wieck A D, Sarov Y, Rangeow I, Naydenov B, Jelezko F, Hell S W and Meijer J 2010 *Small* **6** 2117–21
[14] Ruthstein S, Potapov A, Raitsimring A M and Goldfarb D 2005 *J. Phys. Chem.* B **109** 22843–51
[15] Amemiya Y, Hatakeyarna A and Shimamoto N 2009 *Langmuir* **25** 203–9
[16] Hernando J, Pourrostami T, Garrido J A, Williams O A, Gruen D M, Kromka A, Steinmuller D and Stutzmann M 2007 *Diam. Relat. Mater.* **16** 138–43
[17] Krueger A, Ozawa M, Jarre G, Liang Y, Stegk J and Lu L 2007 *Phys. Status Solidi* a **204** 2881–7
[18] Degen C L 2008 *Appl. Phys. Lett.* **92** 243111
[19] Ziegler J F, Ziegler M D and Biersack J P 2010 *Nucl. Instrum. Methods* B **268** 1818–23
[20] Milov A D, Maryasov A G and Tsvetkov Y D 1998 *Appl. Magn. Reson.* **15** 107–43
[21] Loubser J and Vanwyk J A 1978 *Rep. Prog. Phys.* **41** 1201–48
[22] Samsonenko N D, Zhmykhov G V, Zon V S and Aksenov V K 1979 *J. Struct. Chem.* **20** 951–3
[23] Soltamova A A, Ilyin I V, Baranov P G, Vul' A Y, Kidalov S V, Shakhov F M, Mamin G V, Orlinskii S B, Silkin N I and Salakhov M K 2009 *Physica* B **404** 4518–21
[24] Fionov A V *et al* 2010 *Chem. Phys. Lett.* **493** 319–22
[25] Smith W V, Sorokin P P, Gelles I L and Lasher G J 1959 *Phys. Rev.* **115** 1546–52
[26] de Lange G, Rist D, Dobrovitski V V and Hanson R 2010 arXiv:1008.4395v1 [cond-mat.mes-hall]
[27] Naydenov B, Dolde F, Hall L T, Shin C, Fedder H, Hollenberg L C L, Jelezko F and Wrachtrup J 2011 *Phys. Rev.* B **83** 081201(R)